Reviews

Iron(III) Oxides from Thermal Processes—Synthesis, Structural and Magnetic Properties, Mössbauer Spectroscopy Characterization, and Applications†

Radek Zboril*

Department of Inorganic and Physical Chemistry, Palacky University, Krizkovskeho 10, Olomouc 771 47, Czech Republic

Miroslav Mashlan

Department of Experimental Physics, Palacky University, Svobody 26, Olomouc 771 46, Czech Republic

Dimitris Petridis

Institute of Materials Sciences, NCSR "Demokritos", Athens 15310, Greece

Received April 12, 2001. Revised Manuscript Received December 10, 2001

Structural and magnetic properties, methods of synthesis, and applications of seven iron(III) oxide polymorphs, including rare beta, epsilon, amorphous, and high-pressure forms, are reviewed. Thermal transformations resulting in the formation of iron oxides are classified according to different parameters, and their mechanisms are discussed. ^{57}Fe Mössbauer spectroscopy is presented as a powerful tool for the identification, distinction, and characterization of individual polymorphs. The advantages of Mössbauer spectroscopy are demonstrated with two examples related to the study of the thermally induced solid-state reactions of $Fe_2(SO_4)_3$.

Lead-In

Iron(III) oxide is not only a strategic industrial material but also a convenient compound for the general study of the polymorphism and the mutual polymorphous changes in nanoparticles. The existence of amorphous Fe_2O_3 and four polymorphs (alpha, beta, gamma, and epsilon) has been established. Their discoveries as well as the majority of formation processes are connected with thermal transformations of iron-bearing materials in an oxidizing atmosphere. ^{57}Fe Mössbauer spectroscopy is a unique method that allows one to distinguish and identify individual structural forms, amorphous and nanostructured Fe_2O_3 particles, to analyze their magnetic properties and to study their formation mechanism during thermally induced solid-state reactions. In this review, thermal processes resulted in the Fe_2O_3 formation are classified from different viewpoints and their mechanism is discussed. Applications, structural and magnetic properties, and methods of synthesis of all known forms of iron(III) oxide and their Mössbauer characterization are also summarized. A detailed survey of the properties of rare forms (amorphous Fe_2O_3, β-Fe_2O_3, ϵ-Fe_2O_3, and high-pressure Fe_2O_3) is presented for the first time. With respect to the more known α-Fe_2O_3 and γ-Fe_2O_3, the presented data spring from a series of previous works, including the excellent book by R. M. Cornell and U. Schwertmann.[1] Some unresolved problems, such as the relation between the properties of the original ferrogenous precursor and the structure of the formed iron(III) oxide, or the experimental possibility to distinguish the amorphous Fe_2O_3 from nanostructured γ-Fe_2O_3 or α-Fe_2O_3 particles are discussed. The value of Mössbauer spectroscopy for the characterization of iron(III) oxides produced by thermal processes is demonstrated with two experimental examples taken from our work in the field.

1. Introduction

Iron(III) oxide in all its forms is one of the most used metal oxides with various applications in many scientific and industrial fields. The polymorphic nature of Fe_2O_3 has been known for a long time. Its most frequent polymorphs alpha and gamma have been found in nature as minerals hematite and maghemite. The other polymorphs, beta and epsilon, and nanoparticles of all

† Dedicated to R. L. Mössbauer on the occasion of the 40th jubilee of Nobel Prize presentation.

* To whom correspondence should be addressed. Fax: +420 68 522 5737. E-mail: zboril@risc.upol.cz.

10.1021/cm0111074 CCC: $22.00
Published on Web 02/28/2002

forms have been synthesized and extensively investigated in recent years. Thermal transformations of iron-bearing materials in an oxidizing atmosphere represent a large group of heterogeneous reactions leading to different Fe_2O_3 polymorphs.

^{57}Fe Mössbauer spectroscopy is a very effective technique for the study of the individual Fe_2O_3 forms including amorphous and superparamagnetic nanoparticles. The method presents several important advantages in comparison with other analytical methods in studying polymorphic transformation of Fe_2O_3. For example, its selectivity for iron with no interference from other elements is very important when the iron oxide phase constitutes only a small fraction of the sample. In addition, it is a nondestructive technique suitable for the study of both crystalline and amorphous materials and in this respect it is superior to X-ray diffraction; it is a "fingerprint" method for compound identification, and it allows "in situ" studies to be performed.

The ^{57}Fe Mössbauer spectra are sensitive to the local environment of the iron atoms in the crystal lattice. The hyperfine parameters, isomer shift (*IS*), quadrupole splitting (*QS*), quadrupole shift (ϵ), and magnetic splitting (*B*), provide information about the electronic density and its symmetry and also about the magnetic properties of the ^{57}Fe Mössbauer probe nucleus. Two more quantities extractable from Mössbauer spectra are directly related to lattice vibrations. One is the recoilless resonant fraction and the other the so-called temperature shift (second-order Doppler shift). Valuable information is also obtained from the widths of spectral lines, their relative intensities, and asymmetries and also from the temperature dependence of hyperfine parameters. From the Mössbauer parameters the following information applicable to Fe_2O_3 studies can be obtained: valence state, number, and identification of nonequivalent iron positions in a crystal lattice, type of coordination of iron in its individual positions, level of ordering and stoichiometry, cation substitution, magnetic ordering, and magnetic transition temperature. Following the discovery of the Mössbauer effect,[2] several works have been published describing the fundamentals of Mössbauer spectroscopy.[3−6]

2. Thermal Transformations of Iron-Bearing Materials—Classification and Mechanism

Thermal transformations of iron-bearing materials in an oxidizing atmosphere are processes investigated in the framework of inorganic and physical chemistry, materials chemistry, solid-state chemistry as well as mineralogy, engineering, and industrial chemistry. Many researchers studied the mechanism and kinetics of these complex reactions that can be classified into several groups according to the nature of the initial iron-bearing phase. Examples are as follows: the thermal decompositions of iron(III) compounds including FeO(OH),[7−20] $Fe_2(C_2O_4)_3$,[21−23] $Fe_2(SO_4)_3$,[24−26] $Fe(OH)_3$,[27] $(NH_4)_2Fe(SO_4)_2$,[28] $Fe(OH)SO_4$,[29−32] $NaFe(SO_4)_2$, $Na_3Fe(SO_4)_3$,[33,34] $FeCl_3$,[35,36] $Fe(OH)CO_3$,[37] and $NH_4Fe(C_2O_4)_2$;[38] the thermally induced oxidation of metal iron,[39,40] Fe_3O_4,[41,42] and iron(II) compounds including $FeCl_2$,[43] $FeSO_4$,[43−51] FeS,[52,53] FeC_2O_4,[21,54−56] and iron(II) malate;[57] the thermally induced solid-state reaction of NaCl with $Fe_2(SO_4)_3$;[33,34] the thermal transformations of iron complexes such as iron carbonyl systems,[58−61] iron carboxylate complexes,[62,63] and $(NH_4)_3[Fe(C_2O_4)_3]$;[64] and the conversions of iron-bearing minerals including goethite,[65−71] akaganeite,[72] lepidocrocite,[73,74] siderite,[75] pyrite,[76−82] pyrrhotite,[79,82,83] almandine,[84] biotite,[85,86] phlogopite,[86] vermiculite,[86] illite,[87] or ilmenite.[88−90]

The common point of these processes is the formation of different iron oxides as conversion and/or oxidation products. Calcined samples can contain some of the four iron(III) oxide polymorphs. In the primary nascent phase, iron oxides can be produced in the form of ultrafine particles with sizes of a few nanometers. The crystallization of these amorphous or nanostructured particles as well as the thermally induced polymorphic changes of the less thermally stable polymorphs (β, γ, and ϵ) to α-Fe_2O_3 very often accompany the basic conversion process. Thus, the quantitative and qualitative phase composition of calcination products depends on many factors, such as temperature, time, pressure, rate of gas flow, material thickness, particle size, and the chemical composition and structure of the original material.

The identification of the particular iron oxide form and the mechanism of its formation during thermal transformations are problems not only of scientific but also of technical importance. The mechanism of Fe_2O_3 formation from the iron precursor is very often different. For example, iron(III) oxide can be the product of the following: one-step transformation during thermal outgassing of Fe phases containing SO_3, CO_2, NH_3, or H_2O as in $2FeO(OH) \rightarrow Fe_2O_3 + H_2O$;[7−20] a multistage process during which different intermediate phases are formed, for instance, in the thermal transformation of $FeSO_4 \cdot 7H_2O$ where $FeSO_4 \cdot H_2O$, $FeSO_4$, $Fe(OH)SO_4$, $Fe_2(SO_4)_3$, and other intermediate phases are identified;[43−51] a process accompanied by a change in the iron valency, e.g., $2FeCl_2 + {}^3/_2O_2 \rightarrow Fe_2O_3 + 2Cl_2$;[43] and a process in which the iron(III) oxide is formed as one of the products of a solid-state reaction, for example,

$$30NaCl + 10Fe_2(SO_4)_3 + {}^{15}/_2O_2 \rightarrow 6Na_3Fe(SO_4)_3 + 4NaFe(SO_4)_2 + 5Fe_2O_3 + 4Na_2SO_4 + 15Cl_2$$ [34]

Concerning the relation between the original iron precursor and the crystal structure of the primarily formed Fe_2O_3, no general dependence has been found. In some cases, the Fe_2O_3 particles showed the tendency to maintain the symmetry of the iron environment and some structural or morphological features of the original compound.[1,8,26] Depending on the structure of the primary Fe_2O_3, thermal processes can be divided into four other groups. The structure of the primary product is that of α-Fe_2O_3 (e.g., oxidation of $FeCl_2$),[43] β-Fe_2O_3 (decomposition of $Na_3Fe(SO_4)_3$),[34] and γ-Fe_2O_3 (conversion of lepidocrocite),[1,73,74] or more polymorphs can be formed as primary phases depending on experimental conditions (e.g., conversion of $Fe_2(SO_4)_3$ with possible formation of β-Fe_2O_3 or γ-Fe_2O_3).[91]

Although the thermal transformations of iron-bearing materials can be classified into several of the abovementioned groups, the general description (or the physical model) of each individual reaction group is very difficult. This is connected with specifics of solid-state

reactions and the necessity to fix some of many experimental parameters (heating temperature and time, material purity, weight and thickness, and particle size) to obtain comparable data. To date, the thermal dehydroxylations of FeO(OH) polymorphs (goethite, akaganeite, lepidocrocite, feroxyhyte, and synthetic δ-FeO(OH)) to hematite represent the only subgroup of reactions whose mechanism was successfully described through a general physical model. A common feature of the dehydroxylation of all iron oxyhydroxides is the initial development of microporosity due to the expulsion of water. This is followed by the coalescence of these micropores to mesopores. Pore formation is accompanied by a rise in sample surface area. At higher temperatures, the product sinters and the surface area drops considerably. During dehydroxylation, hydroxy bonds are replaced by oxo bonds and face sharing between octahedra (absent in the FeO(OH) structures, but typical for hematite; see section 4.1) develops and leads to a dense structure. As only one-half of the interstices are filled with cations, some movement of Fe atoms during the transformation is required to achieve the two-thirds occupancy found in hematite.[1]

In concluding this section, it is worth mentioning that certain thermally induced reactions can also be used as methods for the preparation of different iron oxide forms. The right choice of experimental conditions during heat treatment and the postprocessing physical or chemical methods of separation (sedimentation, dissolution, and magnetic separation) play a key role in the synthesis of a particular polymorph.

3. Applications of Iron(III) Oxides and Thermal Processes

Iron(III) oxides are components of many geologically and archeologically important earth samples as well as extraterrestrial materials. Maghemite was found in an Atlantic red clay sample, while hematite and maghemite were found on the Martian surface. Iron oxides and their transformations are the basis for magnetic prospecting of archeological areas.[92] From a technical point of view, the oxides are important materials in several fields. Their utilization as inorganic pigments is well-known.[93−96] Both natural and synthetic pigments are used in the manufacture of red, brown, and black paints or as admixtures, for example, in colored glasses.[97−99] The thermal decomposition of $FeSO_4 \cdot 7H_2O$ is the basis for the red ferric pigment manufacture ("copperas red"). The mechanism of this multistage process is one of the most investigated chemical and industrial processes.

The catalytic properties of iron(III) oxides are used in many important reactions of chemical industry. Iron oxides are one of the catalytic components in the manufacture of styrene by the dehydrogenation of ethylbenzene,[100−103] in Fischer−Tropsch synthesis of hydrocarbons,[104−107] or in Super Claus catalysis.[107] They have been proved effective catalysts for the selective oxidation of polyaromatic hydrocarbons,[108] catalytic burning of fuels,[109] coal liquefaction,[110] and vapor-phase oxidation of benzoic acid to phenol.[111,112] In many cases, Fe_2O_3 catalysts are prepared by thermal processes and their catalytic activity depends on the conditions of preparation.[113]

Iron oxides are also the starting materials in the production of ferrites. Hard ferrites (e.g., $BaFe_{12}O_{19}$ or $SrFe_{12}O_{19}$) are made from Fe_2O_3 by a sintering process. They are used in ceramic, in permanent magnets, in high-density digital storage media, and as antiforgery devices in the magnetic strips of checks and cards. A potential use of these materials may be as "hot sources" in the treatment of certain tumors.[1]

Iron oxides are the most important components of several ores used for the production of iron and steel. On the other hand, high-temperature corrosion of steel involves the formation of some iron oxide phases.[114−117] They are always formed on the surface of steel and sometimes cause serious problems in the fabrication processes. A comprehensive understanding of the formation and transformation mechanism of iron oxides is indispensable for the optimization and control of the manufacture process and for good quality steel.

In the electronics industry, hematite is a potential candidate as a photoanode for possible photoelectrochemical cells.[118] Iron oxides can also be incorporated into the interlayer of layered compounds as semiconductor pillars that show excellent photocatalytic activity.[119]

α-Fe_2O_3 and γ-Fe_2O_3 have attracted much attention as gas sensor materials because their surface resistivities decrease in an atmosphere of combustible gases such as CH_4, C_3H_8, and i-C_4H_{10}.[120−122] In situ studies of conversion electron Mössbauer spectroscopy (CEMS) has significantly contributed to the clarification of the sensing mechanism of these materials.[123]

Owing to their hardness, iron oxides have been used as abrasives and polishing agents. A lightly calcined form of hematite (Jeweler's rouge) is used to polish gold and silver, while a more strongly calcined hematite (crocus) serves to polish brass and steel.[1] Fe_2O_3 has been utilized as high-density coatings for concrete seabed pipelines that bring oil and gas to shore. These coatings stabilize the pipelines on the sea floor and provide protection against physical damage in shallow water.[1]

Small iron oxide particles with diameters of a few nanometers exhibit unique features that strongly differ from those of bulk phases. Electronic, magnetic, and optical properties of superparamagnetic nanoparticles are of fundamental importance in many industrial applications, including the development of new electronic and optical devices, information storage, magnetocaloric refrigeration, color imaging, bioprocessing, ferrofluid technology, or manufacture of magnetic recording media.[124−127] In the latter fields the use of small particles of iron(III) oxides is particularly important. The advantage of using Fe_2O_3 nanoparticles relies on their chemical stability, in contrast to commonly used ultrasmall particles of pure metals (Fe, Co, and Ni). A variety of routes for the synthesis of iron oxide nanoparticles has been reported. Various compositions and morphologies have been attained by oxygen−hydrogen flame pyrolysis,[128,129] electrochemical synthesis,[130] sol−gel methods,[131−133] vaporization−condensation process in a solar furnace,[134] microemulsion techniques,[135] diode sputter deposition,[136] and thermal decomposition of an aerosol upon a heated substrate.[137,138] The final stage in the majority of these preparation methods includes a thermal transformation of iron-bearing material. In some cases, thermal processes can be used as direct routes of synthesis of iron oxide nanoparticles. The simplicity of preparation is the principal advantage of

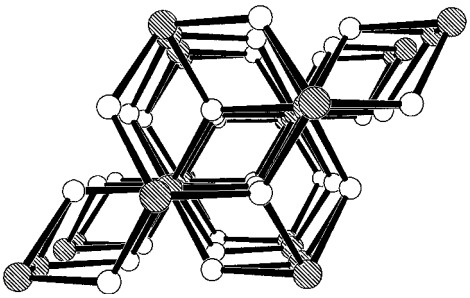

Figure 1. Crystal packing in the structure of α-Fe_2O_3, the view onto (001). Fe, shaded circles; O, white circles.

these direct thermal methods but their application strongly depends on the nature of the initial iron compound. Compounds with a partially amorphous or colloidal character [$Fe_2(C_2O_4)_3$, γ-FeO(OH)] have been used in this direction. Fine maghemite particles are essential components in magnetic recording media for computer hard and floppy disks, credit cards, and audio and video recording tapes.[139] Superparamagnetic iron oxides have also been evaluated in clinical trials as very good contrast agents in magnetic resonance imaging (MRI) for liver, spleen, and other organs.[139,140] Maghemite has been identified in the core of magnetoferritin, which as a biocompatible ferrofluid has considerable potentialities in various medical areas.[141]

4. Iron(III) Oxides

4.1. α-Fe_2O_3 (Hematite). α-Fe_2O_3 is the most researched and most frequent polymorph existing in nature as the mineral hematite. Hematite has a rhombohedrally centered hexagonal structure of the corundum type with a close-packed oxygen lattice in which two-thirds of the octahedral sites are occupied by Fe^{III} ions.[1,92,142,143] The space group $R\bar{3}c$, lattice parameters $a = 5.0356$ Å, $c = 13.7489$ Å, and six formula units per unit cell—these are the basic structural characteristics of α-Fe_2O_3.[144] A noticeable feature of the hematite structure is the arrangement, where the FeO_6 octahedra share edges inside the basal (001) plane and one face in Fe_2O_9 dimers along the [001] c axis (Figure 1).

Hematite shows very interesting magnetic characteristics.[1,92,142,143,145−147] At low temperatures (T < 260 K) it is antiferromagnetic with the spins oriented along the electric field gradient axis. At a temperature known as Morin temperature (T_M), around 260 K, a reorientation of spins by about 90° takes place whereby the spins become slightly canted to each other (by ≈5°), causing the destabilization of their perfect antiparallel arrangement and the development of weak (parasitic) ferromagnetism between Morin and Neel temperature (T_N). The Neel temperature of magnetic transition, at which hematite loses its magnetic ordering and above which shows paramagnetic features, is most frequently reported at 950 K. However, it is necessary to note that the magnetic features of hematite, including the temperature values of magnetic transitions, can be largely influenced by numerous factors, such as pressure, external magnetic fields, lattice defects, presence of impurities, surface phenomena and, in particular, ion substitution, and the size of particles. As the crystallinity of particles decreases, the lowering of the transition temperature becomes evident. In addition, ultrafine

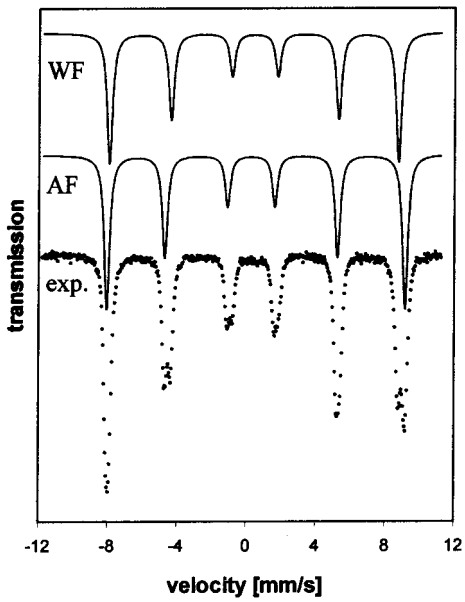

Figure 2. Mössbauer spectrum of the pure synthetic hematite at 260 K, showing the coexistence of both the AF and WF phases.

nanoparticles of α-Fe_2O_3 (<10 nm) show superparamagnetism as a result of the increase of the relaxation time due to the decreasing size of the particles.[148−152]

Mössbauer spectroscopy verifies the mentioned structural and magnetic characteristics. The hyperfine parameters at room temperature, IS_{Fe} (isomer shift related to metalic iron) = 0.37 mm/s, $\epsilon = -0.21$ mm/s, $B = 51.7$ T, can be used to identify hematite in synthetic and natural samples. Moreover, recording the Mössbauer spectra in a wide range of temperatures allows one to study and register the temperature changes in the magnetic features of α-Fe_2O_3, including the magnetic transition temperatures. It is possible to detect not only those transitions related to the loss of magnetic ordering (T_N and T_B, the latter being the blocking temperature of superparamagnetic particles), reflected by a sextet to doublet change in the spectra, but also transitions related to changes in magnetic ordering from antiferromagnetic (AF) to weakly ferromagnetic (WF) states at T_M. This transition is manifested by a change in the parameters of magnetic splitting and, in particular, the quadrupole shift at Morin temperature. While in a WF state at room temperature B is 51.7 T, at T_M it decreases by 0.8 T.[143] The value of the quadrupole shift parameter changes even more markedly. The quadrupole shift parameter ϵ depends on the canting angle φ of the spins with respect to the electric field gradient (E_Q) axis [111], given by $\epsilon = \Delta E_Q(3\cos^2\varphi - 1)/2$ and thus yields values with opposite sign for AF ($\varphi = 0°$) and WF ($\varphi = 90°$) states. In this way both magnetically nonequivalent phases can be probed separately (Figure 2), in contrast to magnetic measurements where mainly the WF phase is observed. Moreover, the Morin transition temperature and the transition width (ΔT_M) can be determined from the temperature response of the relative spectral areas. The Morin transition temperature is defined as that temperature at which the AF contribution of the spectrum is reduced to half of its low-temperature saturation value, whereas ΔT_M corresponds to that temperature region in which the AF and WF portions mutually

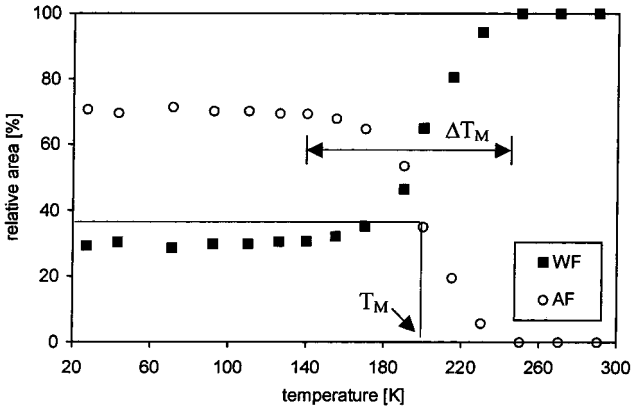

Figure 3. Temperature dependence of the AF and WF relative areas in Mössbauer spectra of hematite substituted by 0.1 wt % Mg.

change (Figure 3). As the values of T_M and ΔT_M are highly sensitive to factors such as particle size, impurities, structural defects, and cation substitution, the Mössbauer spectroscopy is an ideal method for the characterization of natural hematite samples.[92,143,146,147,153]

Concerning the formation and possibilities of preparation of α-Fe_2O_3, it was already mentioned that hematite is one of the final products of thermal conversion of a variety of iron(II) and iron(III) compounds as well as the final product of the thermally induced transformations of other iron oxides. Besides thermal processes, a whole range of methods of hematite synthesis by the "wet way" is known. Hematite can be prepared by hydrolysis of ferric salts in strongly acidic environments (pH = 1−2) at higher temperature (100 °C),[154] by decomposition of iron chelates in alkaline media (pH > 12) in an autoclave,[155] or by transformation of ferrihydrite at pH 7−8 in the presence of $NaHCO_3$ buffer.[154] Accordingly, the preparation of this structural polymorph poses no great problem compared to the preparations of some other polymorphs, in particular, β- and ϵ-Fe_2O_3. Finally, we note that hematite is thermally the most stable polymorph of iron(III) oxides undergoing a thermal reduction to magnetite (Fe_3O_4) at temperatures above 1200 °C.[156]

4.2. β-Fe_2O_3. The beta polymorph of iron(III) oxide has been prepared only synthetically without any mention of natural occurrence. It has a body-centered cubic "bixbyite" structure with $Ia\bar{3}$ space group and two nonequivalent octahedral sites of Fe^{III} ions in the crystal lattice (see Figures 4 and 5). The cubic unit cell with a = 9.404 Å contains 32 Fe^{III} ions, 24 of which have a C_2 symmetry (d position) and 8 a C_{3i} symmetry (b position).[33,157−163] There are 16 formula units per unit cell.

β-Fe_2O_3 is magnetically disordered at room temperature and exhibits paramagnetic behavior, a feature that notably distinguishes it from alpha, gamma, and epsilon polymorphs. The Neel temperature below which β-Fe_2O_3 shows antiferromagnetic features has been observed by different authors to be in the range of 100−119 K.[33,160,163]

The Mössbauer spectra of β-Fe_2O_3 consist of two subspectra, the relative intensities of which are in the ratio 3 to 1, in accordance with the ratio of Fe^{III} in nonequivalent octahedral positions (d/b = 24/8).[33,157,160,163] The parameters of the room temperature (RT) Mössbauer spectrum are IS_{Fe} = 0.37 mm/s and QS = 0.69 mm/s for the d position and IS_{Fe} = 0.37 mm/s and QS = 0.90 mm/s for the b position.[34] The difficulty in distinguishing between nonequivalent cation positions could lead to the fitting of the RT spectrum by one doublet with IS_{Fe} = 0.37 mm/s and QS = 0.75 mm/s.[33] Figure 6 indicates that nonequivalent sites in the structure of β-Fe_2O_3 are better distinguished at low temperatures (below 110 K, in a magnetically ordered state) than at room temperature.[160] In Table 1 the magnetic hyperfine values are shown for both structural positions derived by measuring the Mössbauer spectra at temperatures below T_N.[160]

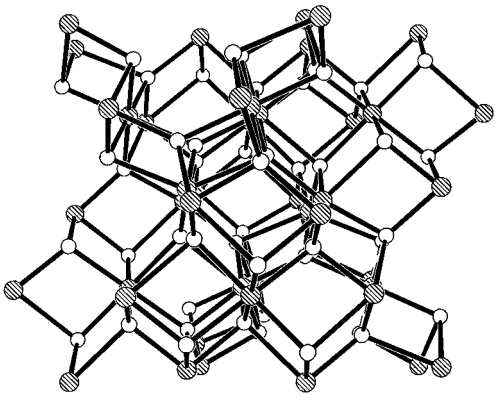

Figure 4. Crystal packing in the structure of β-Fe_2O_3, the view onto (110). Fe, shaded circles; O, white circles.

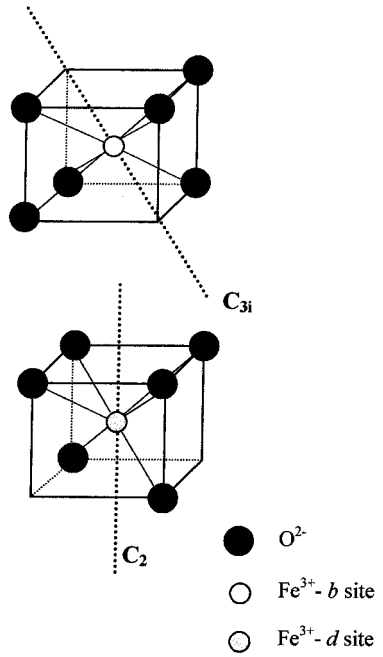

Figure 5. Schematic representation of nonequivalent sites of Fe in the structure of β-Fe_2O_3.

The formation of β-Fe_2O_3 has so far been verified in only a few chemical and physical processes and only two methods of preparation of pure β-Fe_2O_3 have been developed. This rare form of Fe_2O_3 was identified during thermal processes of Mn steel,[164] as an intermediate product in the reduction of hematite by carbon,[165] among the products in a spray pyrolysis of an $FeCl_3$ solution,[159] and during the thermal decomposition of $Fe_2(SO_4)_3$.[26] In a pure state, without the presence of other structural forms, this polymorph was prepared on various sub-

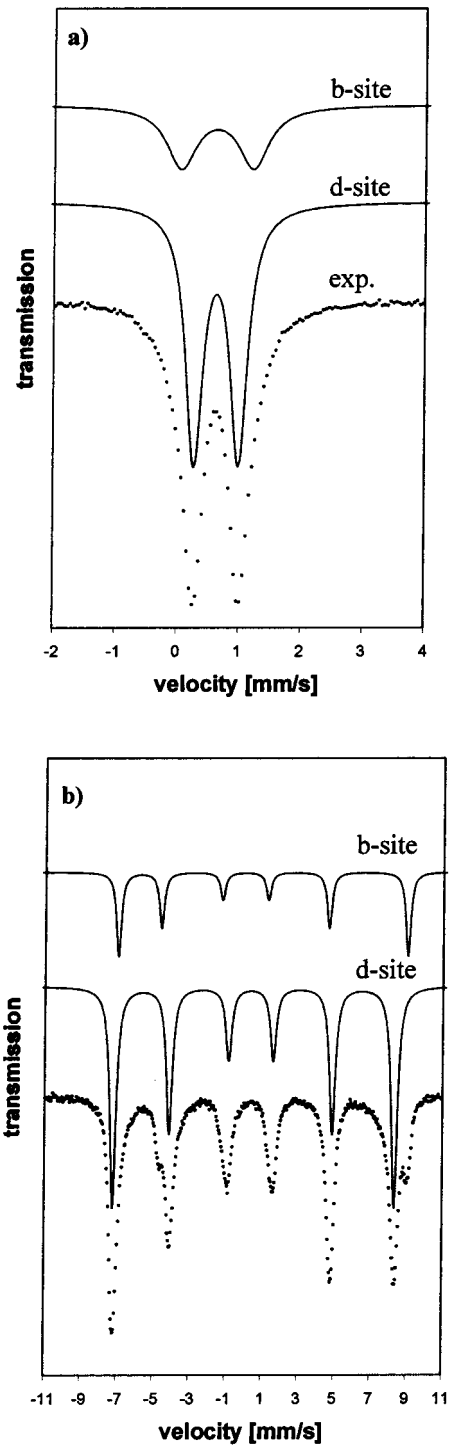

Figure 6. Mössbauer spectrum of β-Fe_2O_3 measured (a) at room temperature and (b) at 20 K.

Table 1. Values of Magnetic Induction for d and b Positions of β-Fe_2O_3

T (K)	*B* (d position) (T)	*B* (b position) (T)
4.1	49.6	51.9
30	47.4	50.2
60	42.9	47.9
80	35.5	41.0
90	30.5	37.3
95	27.1	31.2

strates in the form of a thin film at approximately 300 °C in the atmosphere of O_2 using the chemical vapor deposition method when an organometallic compound was used as a precursor material, most frequently iron(III) acetylacetonate.[157,158,160,161] A second method of synthesis of pure β-Fe_2O_3 is based on its isolation from a reaction mixture during a thermally induced solid-state reaction between NaCl and $Fe_2(SO_4)_3$ in air.[33,34]

β-Fe_2O_3 is thermally metastable and at temperatures around 500 °C is transformed into hematite.[33,157,161−163] It is this instability that complicates its synthesis because hematite is frequently present as a contaminating component.

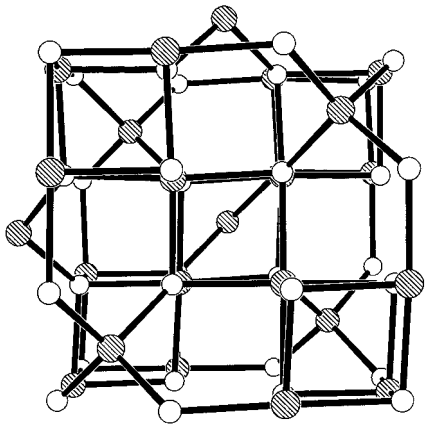

Figure 7. Crystal packing in the structure of γ-Fe_2O_3, the view onto (100). Fe, shaded circles; O, white circles.

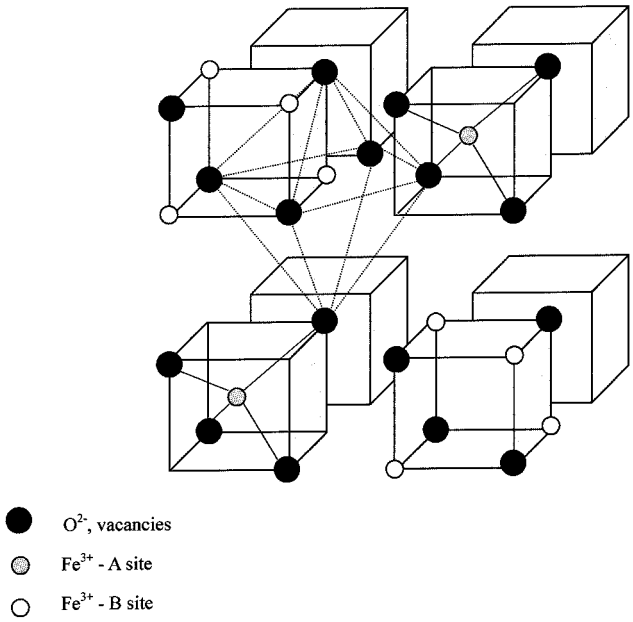

Figure 8. Schematic representation of nonequivalent sites of Fe in the structure of γ-Fe_2O_3.

4.3. γ-Fe_2O_3 (Maghemite). γ-Fe_2O_3 is the second polymorph that occurs in nature as the mineral maghemite. Representation of the maghemite structure is shown in Figure 7. Maghemite is an inverse spinel with a cubic unit cell (a = 8.351 Å, space group $P4_132$).[166] It contains, as in Fe_3O_4, cations in tetrahedral A and octahedral B positions, but there are vacancies (□), usually in octahedral positions, to compensate for the increased positive charge (Figure 8). Stoichiometry can be formally described by the formula $Fe^{A}(Fe_{5/3}\square_{1/3})^{B}O_4$.[1,92,143,146]

Synthetic maghemite often displays a superstructure, which arises as a result of cation and vacancy ordering.

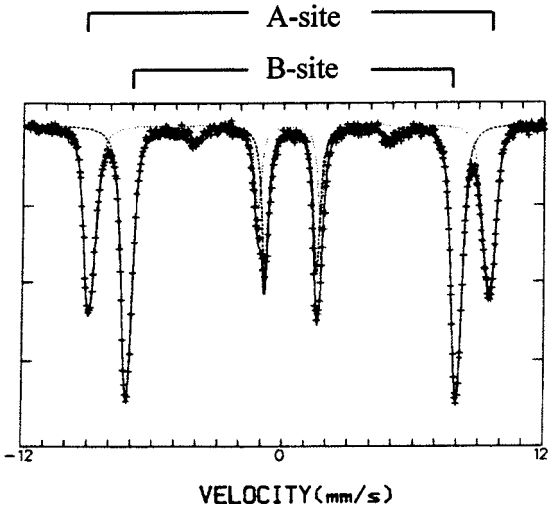

Figure 9. Mössbauer spectrum of a well-crystallized maghemite at 4 K in an external field of 6 T. Reproduced from ref 143.

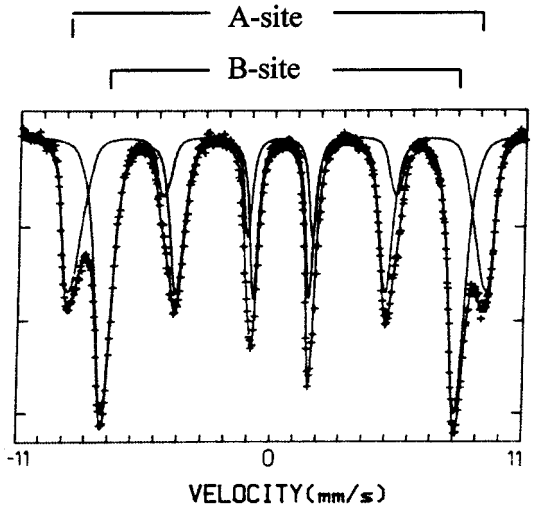

Figure 10. Mössbauer spectrum of a poorly crystalline maghemite at 10 K in an external field of 6 T fitted with two bidimensional $B-\theta$ distributions. Reproduced from ref 13.

This ordering causes a reduction in symmetry from cubic to tetragonal. The tetragonal unit cell has $a = 8.33$ Å and $c = 25.01$ Å.[1] Owing to the spinel structure with two sublattices, maghemite is a typical representative of ferrimagnetic materials that give high susceptibilities to all samples that it is contained in. Its thermal instability disables direct determination of the Curie temperature of magnetic transition. The ultrafine particles of maghemite show, similarly to the hematite, superparamagnetism.[130−135,167−169] γ-Fe_2O_3 was one of the first and experimentally most researched materials for building the theory of superparamagnetic relaxation.

The RT Mössbauer spectrum of maghemite forms a "slightly asymmetric" sextet with the following parameters: $IS_{Fe} = 0.34$ mm/s, $\epsilon = 0$ mm/s, and $B = 50$ T.[146,170] The zero value of the ϵ parameter and the slightly lower value of B are the main features enabling one to identify maghemite in a mixture with hematite ($\epsilon = -0.21$ mm/s, $B = 51.7$ T). In an ideal case and in accordance with the structure of maghemite, the RT Mössbauer spectrum can also be fitted with two overlapping subspectra, with the following parameters: sextet^A $IS_{Fe} = 0.27$ mm/s, $\epsilon = 0$ mm/s, $B = 48.8$ T; sextet^B $IS_{Fe} = 0.41$ mm/s, $\epsilon = 0$ mm/s, $B = 49.9$ T, with the ratio of subspectra areas $A_B/A_A = 5/3$.[92,170] Nevertheless, at room temperature and in a zero external magnetic field, both nonequivalent cation positions in the structure of maghemite are practically indistinguishable, as in the case of the beta polymorph. But by an application of an external magnetic field the contributions of the two sublattices can be separated. The A and B site fields make parallel or antiparallel alignment with respect to the applied field and the resultant fields differ significantly (see Figures 9 and 10). In such Mössbauer spectra the relative areas of the six lines are given by $3:x:1:1:x:3$ where $x = 4 \sin^2 \theta/(1 + \cos^2 \theta)$ with θ being the angle between the magnetic hyperfine field and the gamma ray direction.[171] Thus, lines 2 and 5 vanish when the spins are completely aligned with the external field as demonstrated on the spectrum of a well-crystallized maghemite at 4 K in an external field of 6 T (Figure 9). With decreasing crystallinity of maghemite, the spins do not align perfectly but exhibit canting as shown by the nonzero intensity in lines 2 and 5 of the sextets.[13,143,171] This behavior suggests that the directions of atomic moments are disordered due to spin frustration. The spectra of small-particle (<10 nm) γ-Fe_2O_3 in an external field have been interpreted in terms of spin canting in the work of de Bakker et al.[13] Both hyperfine field B and canting angle θ were assumed to vary and the fitting procedure gave probability distributions of each. A bidimensional "hyperfine field-canting angle" distribution was found to reproduce the experimental line shapes with remarkable adequacy. An example of such a fit is shown in Figure 10.

The common routes of formation that can also be used as methods of preparation of γ-Fe_2O_3 are the thermal dehydration of lepidocrocite, γ-FeO(OH),[18,73,74,154] and the careful oxidation of magnetite, Fe_3O_4.[41,42,154,172] Several other thermally induced syntheses have been developed, for example, thermal decomposition of Fe^{II} malate or other Fe^{II} organic salts,[57] heating of goethite or ferrihydrite in air at 450 °C in the presence of an organic material such as sucrose,[173] and thermal decomposition of $FeOOCH_3$ at 290 °C in a vacuum.[174] Superparamagnetic nanoparticles of γ-Fe_2O_3 can be prepared by thermal transformation of iron(III) oxalate.[21,22] Another approach in the production of variable size γ-Fe_2O_3 nanoparticles is based on the thermal decomposition of iron−carboxylate complexes.[63] Maghemite has also been identified as the primary product of crystallization of amorphous Fe_2O_3.[135] In addition to solid-state preparations, several solution syntheses are known, for example, slow oxidation of a mixed Fe^{II}/Fe^{III} solution at RT and pH = 7,[175] oxidation of Fe^{II} salt solution with air, urotropin, sodium iodate, or sodium nitrate or with air in the presence of a complexing agent such as pyridine or sodium thiosulfate,[176] and electrolysis of Fe^{III} nitrate solution.[177]

γ-Fe_2O_3 is thermally unstable and is transformed to hematite at higher temperatures. The temperature and mechanism of the structural transformation are dependent on experimental conditions and particularly on the size of the maghemite particles. For well-developed crystals of γ-Fe_2O_3 the temperature of transformation

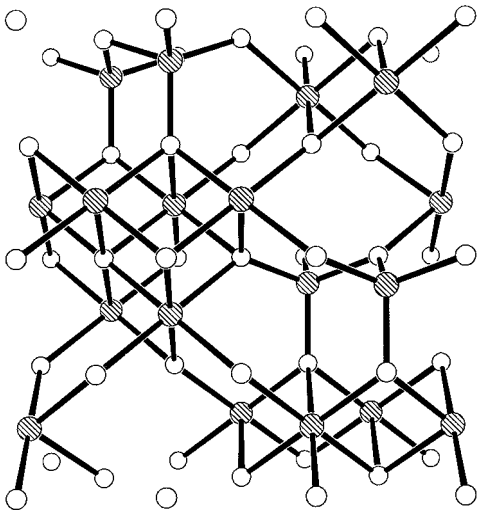

Figure 11. Crystal packing in the structure of ϵ-Fe_2O_3 the view onto (100). Fe, shaded circles; O, white circles.

has been determined at approximately 400 °C and a direct transformation mechanism to α-Fe_2O_3 is expected.[1] In the case of very small particles, a notably higher transformation temperature was noticed with ϵ-Fe_2O_3 being an intermediate of the structural transformation γ-$Fe_2O_3 \rightarrow$ α-Fe_2O_3.[178] According to Tronc et al., the mechanism of transformation to hematite (either directly or via ϵ-Fe_2O_3) is dependent on the degree of particle agglomeration.[178]

4.4. ϵ-Fe_2O_3. ϵ-Fe_2O_3 can be marked as the "youngest" of iron(III) oxides, as its structure was completely described only in 1998 by Tronc et al.[178] However, the first report about the existence of a magnetically ordered polymorph, structurally different from both hematite and maghemite, comes from 1934 when Forestier and Guiot-Guillain first mentioned this oxide.[179] In 1963, Schrader and Bûttner prepared identical material from atomized iron in an electric discharge under oxygen flux and named it ϵ-Fe_2O_3.[39]

ϵ-Fe_2O_3 is orthorhombic with space group $Pna2_1$, lattice parameters $a = 5.095$ Å, $b = 8.789$ Å, $c = 9.437$ Å, and eight formula units per unit cell. The structure derives from a close packing of four oxygen layers. It is isomorphous with $AlFeO_3$, $GaFeO_3$, κ-Al_2O_3, and presumably ϵ-Ga_2O_3. The structure itself (Figure 11) consists of triple chains of octahedra sharing edges and simple chains of tetrahedra sharing corners which run parallel to the *a* direction.[178] In the structure there are three nonequivalent anion (A, B, and C) and four cation (Fe_1, Fe_2, Fe_3, and Fe_4) positions. Position Fe_4 is tetrahedrally coordinated, and the other three positions are octahedrally coordinated (Figure 12).

The comparison of the ϵ-Fe_2O_3 structure with the structures of maghemite and hematite unveils that the former has a number of intermediate features, for example, the anion arrangement (double hexagonal), the fraction of four-coordinated Fe^{III} (25%), and the volume per formula unit (5.29×10^6 pm^3). As in hematite, all oxygen layers contain the same percentage of iron: 0.67 Fe per atom of oxygen. As in maghemite, oxygen sandwiches containing six-coordinated iron alternate with oxygen sandwiches containing six- and four-coordinated iron. Thus, ϵ-Fe_2O_3 may be viewed as an

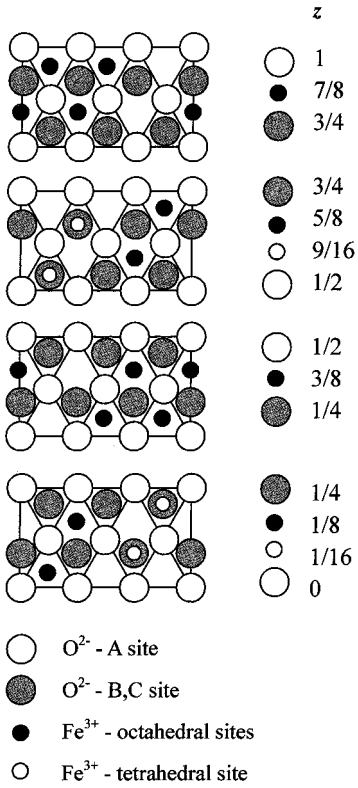

Figure 12. Schematic representation of nonequivalent sites of Fe in the structure of ϵ-Fe_2O_3; the projection of the successive oxygen sandwiches onto (001).

intermediate polymorph between γ-Fe_2O_3 and α-Fe_2O_3.[178] The structure of ϵ-Fe_2O_3 often shows two types of lattice disorders associated with the occupation of cation positions and their orientation. Both types of disorders, observable in X-ray diffraction (XRD) patterns, influence the symmetry of the elementary cell. The differences in the intensities of XRD lines, observed by individual researchers in relation to the method of preparation of ϵ-Fe_2O_3, arise from a different degree of cation ordering. The degree of cation ordering is reflected mainly in the stoichiometric ratio of four- and six-coordinated iron (deviations from the ideal ratio being 3/1).

From the viewpoint of magnetic features, ϵ-Fe_2O_3 is a noncollinear ferrimagnet with Curie temperature near 470 K.[39,178,180,181] The RT Mössbauer spectrum of ϵ-Fe_2O_3 is complex and can be approximated by four sextets corresponding to the individual cation positions with the subspectra areas being nearly equal (Figure 13). The *IS* values indicate three octahedral sites ($IS_{Fe} = 0.37-0.39$ mm/s) and one tetrahedral site of Fe^{III} ($IS_{Fe} = 0.21$ mm/s). Two of the octahedral sites are characterized by close values of a magnetic hyperfine field (≈45 T) causing their overlap. Even so, both positions can be distinguished on the basis of different ϵ values (see Table 2). The third octahedral site exhibits a smaller hyperfine field (≈40 T). In contrast, the value corresponding to the tetrahedral position (≈26 T) is unusually low. The hyperfine parameters of the RT Mössbauer spectrum of ϵ-Fe_2O_3 are summarized in Table 2.[178]

The processes for the ϵ-Fe_2O_3 formation are even poorer than those for the equally rare β-Fe_2O_3. Pure ϵ-Fe_2O_3 has so far not been prepared. In structural mixtures with gamma and alpha polymorphs, ϵ-Fe_2O_3 has been prepared by the oxidation of atomized iron in

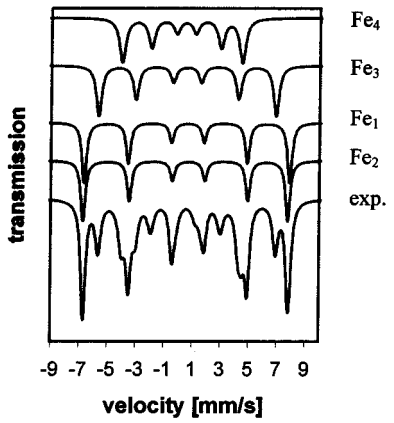

Figure 13. Results of mathematical processing of the RT Mössbauer spectrum of ϵ-Fe_2O_3.

an electric discharge,[39] by a sol−gel method with iron(III) nitrate as the starting material,[133] or by the boiling of an aqueous solution of potassium ferricyanide with sodium hypochlorite and potassium hydroxide with subsequent calcination of the formed precipitate at 400 °C.[180,181] The fact that ϵ-Fe_2O_3 has always been detected together with gamma and alpha polymorphs is, besides the structural data mentioned, yet another indication that ϵ-Fe_2O_3 is an intermediate product in the structural transformation of γ-Fe_2O_3 to α-Fe_2O_3. Definite proof of this hypothesis comes from the work of Tronc et al.,[178] who obtained the epsilon polymorph as the dominating phase (70%) in the direct thermal transformation of ultrafine particles (<10 nm) of γ-Fe_2O_3 well-dispersed in a silica xerogel. The transformation temperature of ϵ-Fe_2O_3 to α-Fe_2O_3 falls within the range, according to the method of preparation, of 500−750 °C.[39,178−181] On the other hand, the particle size of ϵ-Fe_2O_3 prepared by various methods falls within the relatively narrow range of 30−80 nm. So far, a process of formation of large ϵ-Fe_2O_3 crystals has not been described.

4.5. Other Forms of Fe_2O_3. In this part, it is intended to give a brief description and characterization of other Fe_2O_3 forms, the formation of which is not related to thermal transformations of iron compounds in an oxidative atmosphere, but it completes the list of the structural forms of Fe_2O_3 so far known.

4.5.1. Fe_2O_3 Formed during the Thermal Decomposition of β-FeO(OH) in Vacuum. Braun and Gallagher reported in 1972 the discovery of a new tetragonal modification of iron(III) oxide which was, rather inadequately, named "beta", that is, as the case of the cubic modification described in Chapter 4.2.[8] This new form with porous structure was prepared by thermal decomposition of β-FeO(OH) at 170 °C in a vacuum. In 1975 Howe and Gallagher reinvestigated the dehydration mechanism and structure of this iron oxide.[9] They found that the oxide had a defect structure derived from a strong tendency to preserve all structural features of the original compound. Four models of distribution of the anion vacancies in the crystal lattice of the oxide were suggested. These models are in accordance with the tubular structure retained during the dehydration. All internal Fe^{III} ions in the proposed defect structure are five-coordinated while the surface Fe^{III} ions are four-coordinated. The Neel temperature of the magnetic transition lies between 300 and 380 K and the average value of magnetic induction of the magnetic field at 4.2 K is 49.5 T. The RT Mössbauer spectrum of this oxide shows the superposition of magnetically split and paramagnetic components. The spectrum measured above Neel temperature comprises a wide asymmetric doublet with $QS = 1.0$ mm/s and IS_{Fe} (extrapolated to 295 K) = 0.31 mm/s. Except from the dehydration of β-FeO(OH) there is no other known process for the formation of this defect structure of iron(III) oxide.

4.5.2. High-Pressure Form of Fe_2O_3. A number of papers have focused on the study of a high-pressure form of α-Fe_2O_3.[182−188] Reid and Ringwood[182] predicted the existence of perovskite-type Fe_2O_3 at pressures between 60 and 120 GPa and in shock wave experiments. Later, the phase transformation of α-Fe_2O_3 was observed under the static pressure conditions using diamond anvil cells, and the structure of high-pressure modification was studied using primarily XRD[183,184] and Mössbauer spectroscopy.[184−187] Stan Olsen et al. carried out high-pressure XRD experiments on hematite using synchrotron radiation and observed the structural transformation at 55 GPa.[188] The transformation is reversible and the structure reverts to that of α-Fe_2O_3 upon release of pressure. The researchers showed that the high-pressure form of α-Fe_2O_3 is orthorhombic of the $GdFeO_3$ type with the *Pbnm* space group and lattice parameters at 60 GPa: $a = 4.59$ Å, $b = 4.97$ Å, $c = 6.68$ Å, $Z = 4$. The volume per formula unit in this orthorhombic structure is 10% smaller than that in α-Fe_2O_3. It is suggested that this volume change arises from a combination of a valence change and high-spin/low-spin transition. The RT Mössbauer spectrum consists of two subspectra indicative of the existence of two different iron positions in the structure. Syono et al. determined the following RT spectrum parameters measured at 60 GPa: $IS_{Fe} = 0.40$ mm/s, $\epsilon = 1.15$ mm/s, and $B = 32.4$ T for the magnetically ordered component (sextet) and $IS_{Fe} = 0.07$ mm/s and $QS = 0.89$ mm/s for the paramagnetic component (doublet).[185]

4.5.3. Amorphous Fe_2O_3. According to Ayyub et al.,[135] an amorphous iron(III) oxide is formed from very small particles, <5 nm in diameter. Van Diepen and Popma suggest that, in amorphous Fe_2O_3, Fe^{III} ions are surrounded by oxygen octahedra with the respective symmetry axes randomly orientated in a nonperiodic lattice.[137] Results obtained from Mössbauer spectroscopy and magnetic susceptibility measurements show that amorphous Fe_2O_3 is paramagnetic at temperatures above $T_N = 80$ K with a magnetic moment of 2.5 μ_B per atom of iron.[136,137] This unexpectedly low value (the usual value for $Fe^{III} \sim 5\ \mu_B$) is ascribed to the formation of clusters.[137] The RT Mössbauer spectrum displays a paramagnetic doublet, with $IS_{Fe} = 0.33-0.35$ mm/s and $QS = 0.95-1.1$ mm/s.[135−137,189] Ayyub et al. further reported that the RT Mössbauer spectrum of the amorphous Fe_2O_3 contains an additional singlet component ($IS_{Fe} = 0.12-0.16$ mm/s), constituting approximately 25% of the overall area of the spectrum.[135] The origin of this singlet still remains unexplained. The value of magnetic induction of the magnetic field at 4.2 K is reported to be approximately $B = 47$ T.[136,137] One of the principal problems in the study of ultrafine particles of Fe_2O_3 is the experimental difficulty of distinguishing between an amorphous state of Fe_2O_3 and superpara-

Table 2. Parameters of the RT Mössbauer Spectrum for ϵ-Fe_2O_3

octahedral sites			tetrahedral site
Fe_1	Fe_2	Fe_3	Fe_4
$IS_{Fe} = 0.37$ mm/s	$IS_{Fe} = 0.39$ mm/s	$IS_{Fe} = 0.38$ mm/s	$IS_{Fe} = 0.21$ mm/s
$\epsilon = -0.19$ mm/s	$\epsilon = -0.06$ mm/s	$\epsilon = 0$ mm/s	$\epsilon = -0.07$ mm/s
$B = 45.0$ T	$B = 45.2$ T	$B = 39.5$ T	$B = 26.2$ T

magnetic nanoparticles of γ- or α-Fe_2O_3. Heiman and Kazama[136] prefer the interpretation that amorphous Fe_2O_3 shows specific magnetic behavior, which is distinct from superparamagnetism. Their suggestion is based on Mössbauer data, listing two differences in the behavior of amorphous and superparamagnetic particles. First, while in the case of amorphous particles it is possible to observe even small decreases in the intensity of the internal magnetic field (H_{INT}) with increasing temperature, the value of H_{INT} remains relatively unchanged with superparamagnetic particles and only the area of the sextet component decreases. The second difference arises from the comparison of the magnetically split spectra (measured below T_N or T_B, respectively) of amorphous and superparamagnetic particles, with higher values of the width of spectral lines corresponding to amorphous particles. The amorphous iron(III) oxide can be prepared by a three-stage microemulsion technique ending with a calcination of the precipitated $Fe(OH)_3$ at 250 °C,[135] by a surface oxidation of monolayers of $Fe(CO)_5$ adsorbed on graphite,[189] and by thermal decomposition of aerosol generated by atomization of an $FeCl_3$ solution in butyl acetate.[137] The thermally induced crystallization of amorphous Fe_2O_3 is carried out in two steps. Ayyub et al. detected two exothermic effects on the DTA curve.[135] The first at approximately 290 °C was ascribed to the formation of γ-Fe_2O_3 and the other at 400 °C to the structural transformation of γ-Fe_2O_3 to α-Fe_2O_3. However, van Diepen and Popma prefer the formation of metastable β-Fe_2O_3 as the primary crystallization phase.[137]

5. Mössbauer Spectroscopy in Studies of Iron(III) Oxides Formed during Thermal Processes

The advantages of Mössbauer spectroscopy for the study of iron oxides formed during thermal transformations of ferrogenous sources were described in previous sections. In this section we wish to demonstrate that Mössbauer spectroscopy can be a powerful tool for the identification of iron(III) oxides as well as for the elucidation of the manner of their formation. The examples are taken from our work in the field. The first, related to the thermal decomposition of $Fe_2(SO_4)_3$, shows in a unique way the polymorphic character of iron(III) oxide. In addition, the value of Mössbauer spectroscopy for the elucidation of the reaction mechanism in the thermally induced solid-state reaction between NaCl and $Fe_2(SO_4)_3$ is presented.

5.1. Thermal Conversion of $Fe_2(SO_4)_3$.[26,91] The mechanism of thermal decomposition of $Fe_2(SO_4)_3$ in air strongly depends on temperature. At 520 °C, near the minimum conversion temperature, superparamagnetic nanoparticles of γ-Fe_2O_3 are formed as a primary conversion product. A broad (fwhm = 0.72 mm/s) superparamagnetic doublet with $IS_{Fe} = 0.37$ mm/s and $QS = 1.0$ mm/s is dominant in RT spectra of samples heated for shorter times at 520 °C. With increasing the heating time, the nanoparticles of γ-Fe_2O_3 are gradually transformed into the thermally stable α-Fe_2O_3 via intermediate ϵ-Fe_2O_3 formation. Four nonequivalent sites of iron in the structure of ϵ-Fe_2O_3 result in the very specific Mössbauer spectrum, which allows easy identification of this polymorph. Therefore, the mechanism of the thermal conversion of $Fe_2(SO_4)_3$ at 520 °C can be described through the model of the consequent solid-state transformations: $Fe_2(SO_4)_3 \rightarrow \gamma$-$Fe_2O_3 \rightarrow \epsilon$-$Fe_2O_3 \rightarrow \alpha$-$Fe_2O_3$. The RT Mössbauer spectrum of the interesting mixture of three Fe_2O_3 polymorphs formed by heating $Fe_2(SO_4)_3$ at 520 °C for 5 h is shown in Figure 14a.

Increasing the calcination temperature to 600 °C changes the reaction mechanism. Gamma and epsilon polymorphs were not detected in thermally treated samples. However, the narrow doublet (fwhm = 0.25 mm/s) with parameters corresponding to β-Fe_2O_3, $IS_{Fe} = 0.37$ mm/s and $QS = 0.74$ mm/s, was observed in the RT Mössbauer spectra of samples heated at 600 °C (Figure 14b). With an increase in the heating time, β-Fe_2O_3 is also transformed into hematite. This polymorphic change is proven by a gradual increase of the sextet areas in the Mössbauer spectra. It is evident that this second mechanism of thermal decomposition of $Fe_2(SO_4)_3$ occurring at 600 °C can be expressed as a result of the transformations: $Fe_2(SO_4)_3 \rightarrow \beta$-$Fe_2O_3 \rightarrow \alpha$-$Fe_2O_3$. In summary, the thermal conversion of $Fe_2(SO_4)_3$ represents a unique solid-state process during which four polymorphs of Fe_2O_3 are formed and Mössbauer spectroscopy is an elegant technique to characterize the different phases and transformation mechanisms.

5.2. Thermally Induced Solid-State Reaction of NaCl with $Fe_2(SO_4)_3$ in Air.[34] Understanding the mechanism of solid-state reactions in cases where two or more solid reactants are involved is not easy. In such case it is necessary both to determine the molar ratio of reactants and to identify and quantify all reaction products, including the gaseous phases. Many experiments and different experimental techniques are needed to obtain the required information. ^{57}Fe Mössbauer spectroscopy can significantly contribute to the study of such reactions where some solid reactants are Fe-bearing compounds. To demonstrate it, we present the example of the thermally induced solid-state reaction between NaCl and $Fe_2(SO_4)_3$ in air.

Experimental determination of the initial molar ratio of NaCl and $Fe_2(SO_4)_3$ was performed indirectly on the basis of the identification and quantification of reaction products. The mixture of sulfate and chloride in an arbitrarily selected molar ratio (1/1) was heated in air at 400 °C for 5 h and analyzed. β-Fe_2O_3, $Na_3Fe(SO_4)_3$, $NaFe(SO_4)_2$, and Na_2SO_4 were unambiguously identified as solid reaction products by XRD. The excess of the initial iron(III) sulfate and therefore low weight per-

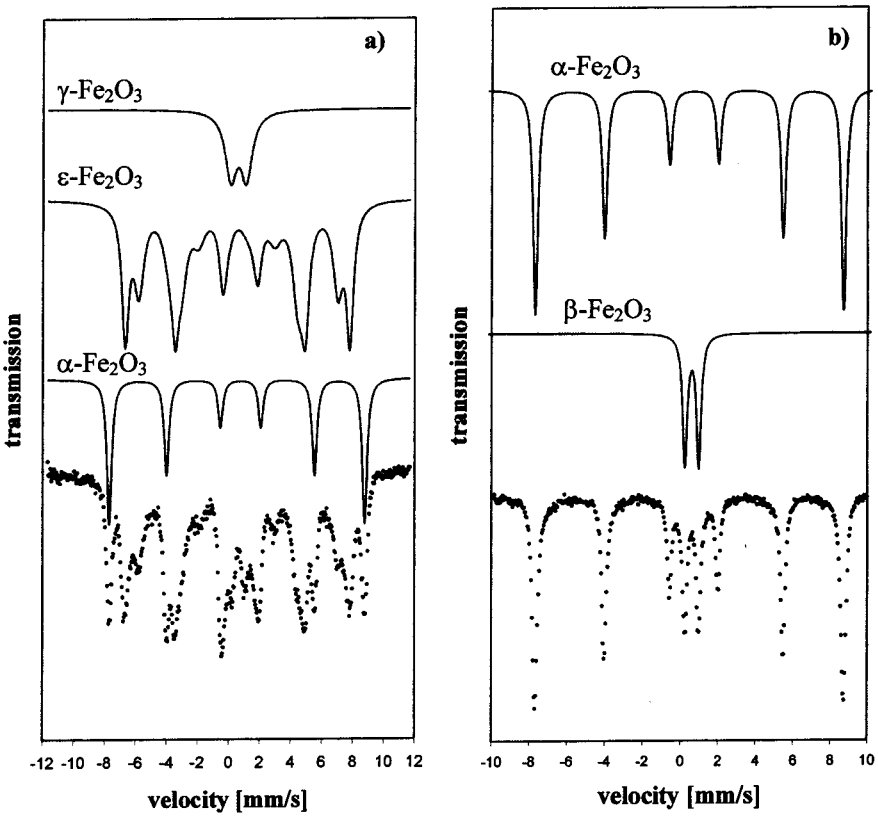

Figure 14. RT Mössbauer spectra of iron(III) oxides prepared by the thermal conversion of $Fe_2(SO_4)_3$ in air: (a) at 520 °C for 5 h; (b) at 600 °C for 2 h.

centages of some products complicated the correct quantitative determination of products by XRD, a problem suitable for ^{57}Fe Mössbauer spectroscopy. To react the entire $Fe_2(SO_4)_3$, a sample with excess NaCl (molar ratio 5/1) was heated at the same conditions as in the previous case. Three iron phases were revealed by Mössbauer spectroscopy results (Figure 15). The same isomer shift (0.46 mm/s) was observed for the two sulfates phases. The hexagonal $Na_3Fe(SO_4)_3$ corresponds to a doublet with a very low value of quadrupole splitting (0.05 mm/s). The monoclinic $NaFe(SO_4)_2$ shows the doublet with a higher *QS* (0.4 mm/s) as a result of lower symmetry of the iron environment. The third doublet with significantly lower IS_{Fe} (0.37 mm/s) was assigned to β-Fe_2O_3. The percentages of the subspectra areas indicated that the products contained approximately 50% ferric ions in the form of β-Fe_2O_3, 30% in the form of $Na_3Fe(SO_4)_3$, and 20% in the form of $NaFe(SO_4)_2$. The ratio of ferric ions of 5:3:2 corresponds to the molar ratio of Fe_2O_3:$Na_3Fe(SO_4)_3$:$NaFe(SO_4)_2$ = 5:6:4 (Fe_2O_3 contains two ferric ions in contrast to both double sulfates). On the basis of these results, quantitative data for other phases were calculated and the following reaction mechanism was suggested:

$$30NaCl + 10Fe_2(SO_4)_3 + {}^{15}/_2O_2 \rightarrow 6Na_3Fe(SO_4)_3 + 4NaFe(SO_4)_2 + 5\beta\text{-}Fe_2O_3 + 4Na_2SO_4 + 15Cl_2$$

To confirm the suggested reaction mechanism, NaCl and $Fe_2(SO_4)_3$ were heated in a calculated molar ratio (3/1) at 400 °C for 5 h. The obtained phase mixture did not contain reactants, in accordance with XRD and Mössbauer spectroscopy results, and the weight decrease

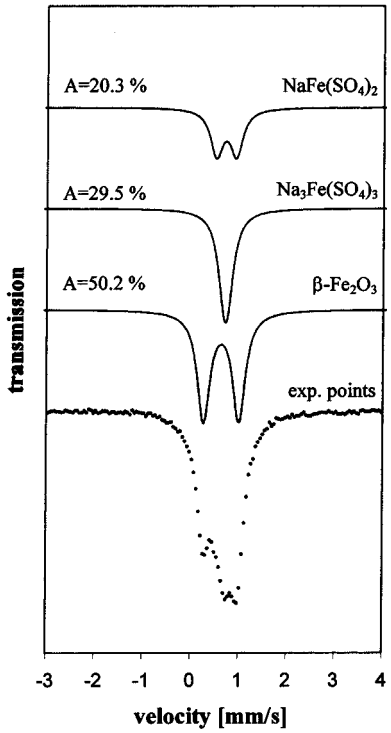

Figure 15. RT Mössbauer spectrum of the products of thermally induced (400 °C) solid-state reaction between $Fe_2(SO_4)_3$ and NaCl in air. *A*, relative spectrum area.

determined from isothermal TG measurements (14.3%) corresponded closely to the suggested reaction mechanism. This example shows that ^{57}Fe Mössbauer spectroscopy is an excellent tool in studying the mechanism

of solid-state reactions where some solid reactants are Fe-bearing compounds.

6. Summary and Outlook

During recent years, considerable progress has been made in the synthesis and study of the structural and magnetic properties of different forms of iron(III) oxide. New knowledge with respect to the properties of superparamagnetic nanoparticles of iron(III) oxide led to their expansion in various industrial fields. The last two decades also brought the new view on the mechanism of many thermal processes ending by the Fe_2O_3 formation. The advances so far achieved are the result of extensive experimental investigations whose essential part is today ^{57}Fe Mössbauer spectroscopy. However, we can expect that experimental scientists will be pressed to solve several unsolved problems in the future. Why has there not been success in synthesizing the pure ϵ-Fe_2O_3 or in preparing the large crystallites of this form up to now? How to explain the controversial magnetic behavior and transformation mechanism of amorphous Fe_2O_3? What role does particle size play in the mechanism of isochemical thermally induced structural transformations of iron(III) oxides? How many other structural forms are waiting to be discovered? The step by step larger society of "iron oxide scientists" as well as the rapid progress in experimental techniques (synchrotron methods, modern microscopic techniques—scanning tunneling microscopy, and atomic force microscopy) give hope that answers to these issues will be known soon.

From the viewpoint of theoretical physics and chemistry, the main objectives will be to find the general physical model for the individual types of thermally induced solid-state reactions and to explain the narrow relation between the properties (structure, particles size, and morphology) of the original thermally treated materials and the properties of the formed iron(III) oxide. Nevertheless, the theoretical description of the mechanism of the thermal dehydroxylation of iron(III) oxyhydroxides is clear evidence that this gap in solid-state chemistry can also be filled soon.

Acknowledgment. Financial support from the Grant Agency of The Czech Republic under Projects 202/00/0982 and 202/00/D091 and through a NATO Linkage Grant HTECH LG 973515 is acknowledged.

References

(1) Cornel, R. M.; Schwertmann, U. *The Iron Oxides. Structure, Properties, Reactions and Uses*; VCH: Weinheim, 1996.
(2) Mössbauer, R. L. *Physik* **1958**, *151*, 124.
(3) Wertheim, G. K. *Mössbauer Effect, Principles and Applications*; Academic Press: New York, 1964.
(4) Goldanskii, V. I.; Herber, R. H. *Chemical Application of Mössbauer Spectroscopy*; Academic Press: New York, 1968.
(5) Cranshaw, T. E.; Dale, B. W.; Longworth, G. O.; Johnson, C. E. *Mössbauer Spectroscopy and Its Applications*; Cambridge University Press: Cambridge, 1985.
(6) Schatz, G.; Weidinger, A.; Gardner, J. A. *Nuclear Condensed Matter Physics (Nuclear Methods and Applications)*; John Wiley & Sons: Chichester, 1996.
(7) Dézsi, I.; Keszthelyi, L.; Kulgawczuk, D.; Molnár, B.; Eissa, N. A. *Phys. Status Solidi* **1967**, *22*, 617.
(8) Braun, H.; Gallagher, K. J. *Nature, Phys. Sci.* **1972**, *240*, 13.
(9) Howe, A. T.; Galagher, K. J. *J. Chem. Soc., Faraday Trans. 1* **1975**, *71*, 22.
(10) Barb, D.; Diamandescu, L.; Mihaila-Tarabasanu, D.; Rusi, A.; Morariu, M. *Hyperfine Interact.* **1990**, *53*, 285.
(11) Sakash, G. S.; Solntseva, L. S.; Plyusnina, I. I. *Zh. Prikl. Spektrosk.* **1972**, *16*, 300.
(12) Cornell, R. M. *Clay Miner.* **1983**, *18*, 209.
(13) de Bakker, P. M. A.; de Grave, E.; Vandenberghe, R. E.; Bowen, L. H. *Hyperfine Interact.* **1990**, *54*, 493.
(14) Ishikawa, T.; Sakata, W.; Kandori, K. *Colloid Surf. A* **1998**, *136*, 183.
(15) Ishikawa, T.; Cai, W. Y.; Kandori, K. *J. Chem. Soc., Faraday Trans.* **1992**, *88*, 1173.
(16) Ishikawa, T.; Yasukawa, A.; Orii, R. *J. Chem. Soc., Faraday Trans.* **1994**, *90*, 2567.
(17) Jimenes Mateos, J. M.; Macioas, M.; J. Morales, J. *J. Mater. Sci.* **1990**, *25*, 5207.
(18) Naono, H.; Nakai, K. *J. Colloid Interface Sci.* **1989**, *128*, 146.
(19) Diamandascu, L.; Milhaila-Tarabasanu, D.; Calogero, S. *Mater. Chem. Phys.* **1997**, *48*, 170.
(20) Yapp, C. J. *Geochim. Cosmochim. Acta* **1990**, *54*, 229.
(21) Suzdalev, I. P.; Krupyianskii, Y. F. *Kinet. Katal.* **1969**, *10*, 1255.
(22) Krupyianskii, Y. F.; Suzdalev, I. P. *Sov. Phys. JETP* **1974**, *38*, 859.
(23) Galwey, A. K.; Mohamed, M. A. *Thermochim. Acta* **1993**, *213*, 279.
(24) Coombs, P. G.; Munir, Z. A. *J. Therm. Anal.* **1989**, *35*, 967.
(25) Kamel, A. H.; Abdallah, A. M. *J. Appl. Chem. Biotechnol.* **1972**, *22*, 599.
(26) Zboril, R.; Mashlan, M.; Krausova, D.; Pikal, P. *Hyperfine Interact.* **1999**, *121−122*, 497.
(27) Au-Yeung, S. C. F.; Denes, G.; Greedan, J. E.; Eaton, D. R.; Birchall, T. *Inorg. Chem.* **1984**, *23*, 1513.
(28) Heilmann, I.; Knudsen, J. M.; Olsen, N. B.; Buras, B.; Staun Olsen, J. *Solid State Commun.* **1974**, *15*, 1481.
(29) Music, S.; Vertes, A.; Simmons, G. W.; Czako-Nagy, I.; Leidheiser, H. *Radiochem. Radioanal. Lett.* **1981**, *49*, 315.
(30) Turlakov, V. N.; Dyakonov, L. I.; Sheinkman, A. I. *Zh. Prikl. Khim.* **1979**, *52*, 1696.
(31) Ivanova, G. V.; Sokolova, V. I.; Baikova, L. A.; Kalinichenko, I. I.; Nikonenko, E. A. *Zh. Neorg. Khim.* **1979**, *24*, 2346.
(32) Pekarskaya, G. V.; Sokolov, V. I.; Kalinichenko, I. I. *Zh. Neorg. Khim.* **1981**, *26*, 1221.
(33) Ikeda, Y.; Takano, M.; Bando, Y. *Bull. Inst. Chem. Res., Kyoto Univ.* **1986**, *64*, 249.
(34) Zboril, R.; Mashlan, M.; Krausova D. The Mechanism of β-Fe_2O_3 Formation by Solid-State Reaction between NaCl and $Fe_2(SO_4)_3$. In *Mössbauer Spectroscopy in Materials Science*; Miglierini, M., Petridis, D., Eds.; Kluwer Academic Publishers: Dordrecht, 1999; pp 49−56.
(35) Kanungo, S. B.; Mishra, S. K. *J. Therm. Anal.* **1996**, *46*, 1487.
(36) Kanungo, S. B.; Mishra, S. K. *J. Therm. Anal.* **1997**, *48*, 385.
(37) Markov, L.; Blaskov, V.; Klissurski, D. *J. Mater. Sci.* **1990**, *25*, 3096.
(38) Hussein, G. A. M.; Ismail, H. M.; Attyia, K. M. E. *J. Anal. Appl. Pyrol.* **1995**, *31*, 157.
(39) Schrader, R.; Büttner, G. *Z. Anorg. Allg. Chem.* **1963**, *320*, 220.
(40) Gleitzer, C.; Nowotny, J.; Rekas, M. *Appl. Phys. A* **1991**, *53*, 310.
(41) Feitknecht, W.; Mannweiler, U. *Helv. Chim. Acta* **1967**, *50*, 570.
(42) Gallagher, K. J.; Feitknecht, W.; Mannweiller, U. *Nature* **1968**, *217*, 1118.
(43) Vertes, A.; Zsoldos, B. *Acta Chim. Acad. Sci. Hung.* **1970**, *65*, 261.
(44) Neto, K. S.; Garg, V. K. *J. Inorg. Nucl. Chem.* **1975**, *37*, 2287.
(45) Kamel, A. H.; Sawires, Z.; Khalifa, H.; Saleh, S. A.; Abdallah, A. M. *J. Appl. Chem. Biotechnol.* **1972**, *22*, 591.
(46) Bristoti, A.; Kunrath, J. I.; Viccaro, P. J.; Bergter, L. *J. Inorg. Nucl. Chem.* **1975**, *37*, 1149.
(47) Prasad, T. P. *J. Therm. Anal.* **1986**, *31*, 553.
(48) Pelovski, Y.; Petkova, V.; Nikolov, S. *Thermochim. Acta* **1996**, *274*, 273.
(49) Gallagher, P. K.; Johnson, D. W.; Schrey, F. *J. Am. Ceram. Soc.* **1970**, *53*, 666.
(50) Johnson, D. W.; Gallagher, P. K. *J. Phys. Chem.* **1971**, *75*, 1179.
(51) Zboril, R.; Maslan, M.; Krausova, D.; Grambal, F. *Czech. J. Phys.* **1997**, *47*, 565.
(52) Banerjee, A. C. *Indian J. Chem. Sect. A* **1976**, *14*, 845.
(53) Coombs, P. G.; Munir, Z. A. *Metall. Trans. B—Process Metall.* **1989**, *20*, 661.
(54) Kong, Y.; Xue, D.; Li, F. *Phys. Status Solidi A* **1996**, *154*, 553.
(55) Mohamed, M. A.; Galwey, A. K. *Thermochim. Acta* **1993**, *213*, 269.
(56) Brown, R. A.; Bevant, S. C. *J. Inorg. Nucl. Chem.* **1966**, *28*, 387.
(57) Nikumbh, A.; Lutkar, A. A.; Phadke, M. M. *Thermochim. Acta* **1993**, *219*, 269.
(58) Gallagher, P. K.; Sinclaor, W. R.; Fastnacht, R. A.; Luongo, J. P. *Thermochim. Acta* **1974**, *8*, 141.
(59) Hu, Z. Q.; Zhao, X. Q.; Liang, Y. *Nanostruct. Mater.* **1994**, *4*, 397.
(60) Tannenbaum, R.; Flenniken, C. L.; Goldberg, E. P. *J. Polym. Sci., Part B: Polym. Phys.* **1990**, *28*, 2421.

(61) Pavlyukhina, L. A.; Odegova, G. V.; Pavlyukhin, Y. T. *Dokl. Khim.* **1996**, *350*, 225.
(62) Uekawa, N.; Kaneko, K. *J. Mater. Res.* **1999**, *14*, 2002.
(63) Lanjewar, R. B.; Garg, A. N. *Indian J. Chem. A* **1991**, *30*, 350.
(64) Ezahri, M.; Coffy, G.; Mentzen, B. F. *Eur. J. Solid State Inorg. Chem.* **1995**, *32*, 237.
(65) Pelino, M.; Toro, L.; Petroni, M. *J. Mater. Sci.* **1989**, *24*, 409.
(66) Pomies, M. P.; Menu, M.; Vignaud, C. *J. Eur. Ceram. Soc.* **1999**, *19*, 1605.
(67) Dekkers, M. J. *Geophys. J. Int.* **1990**, *103*, 233.
(68) Gualtieri, A. F.; Venturelli, P. *Am. Mineral.* **1999**, *84*, 895.
(69) Pomies, M. P.; Morin, G.; Vignaud, C. *Eur. J. Solid State Inorg. Chem.* **1998**, *35*, 9.
(70) Rosler, M.; Held, E.; Hofmeister, H. *J. Magn. Magn. Mater.* **1993**, *120*, 48.
(71) Diamandescu, L.; Mihaila-Tarabasanu, D.; Felder, M. *Mater. Lett.* **1993**, *17*, 309.
(72) Cornell, R. M.; Givanoli, R. *Clay. Clay Miner.* **1991**, *39*, 144.
(73) de Bakker, P. M. A.; Bowen, L. H.; Pollard, R. J. *Phys. Chem. Miner.* **1991**, *18*, 131.
(74) Criado, J. M.; Chopra, G. S.; Real, C. *Chem. Mater.* **1999**, *11*, 1128.
(75) Jagtap, S. B.; Pande, A. R.; Gokarn, A. N. *Int. J. Miner. Process.* **1992**, *36*, 113.
(76) Hong, Y.; Fegley, B., Jr. *Ber. Bunsen-Ges. Phys. Chem.* **1997**, *101*, 1870.
(77) Kirilov, P. P.; Gruncharov, I. N.; Pelovski, Y. G. *Thermochim. Acta* **1994**, *244*, 79.
(78) Luganov, V. A.; Shabalin, V. I. *Can. Metall. Quart.* **1994**, *33*, 169.
(79) Dunn, J. G.; Mackey, L. C. *J. Therm. Anal.* **1993**, *39*, 1255.
(80) Zhizhaev, A. M.; Kim, A. P. *J. Min. Sci.* **1992**, *28*, 295.
(81) Safiulin, N. S.; Gitis, E. B. *Tr. Nauch.-Issled. Inst. Osn Khim.* **1969**, *19*, 110.
(82) Paulik, F.; Arnold, M. *J. Therm. Anal.* **1993**, *39*, 1089.
(83) Steger, H. F. *Chem. Geol.* **1982**, *35*, 281.
(84) Mašláň, M.; Šindelář, Z.; Martinec, P.; Chmielová, M.; Kholmetskii, A. L. *Czech. J. Phys.* **1997**, *47*, 571.
(85) Hoog, C. S.; Meads, R. E. *Mineral. Magn.* **1975**, *40*, 89.
(86) Tripathi, R. P.; Chendra, U.; Chandra, R.; Lokanathan, S. *J. Inorg. Nucl. Chem.* **1978**, *40*, 1293.
(87) Wagner, U.; Knorr, W.; Forster, A.; Murad, E.; Salazar, R.; Wagner, F. E. *Hyperfine Interact.* **1988**, *41*, 855.
(88) Manrique, M.; Figueira, T.; Taylor, P. R. *Astrophys. Space Sci.* **1997**, *256*, 499.
(89) Briggs, A. R.; Sacco, A., Jr. *Metall. Trans. A-Phys. Metall. Mater. Sci.* **1991**, *24*, 301.
(90) Tilly, J.; Lewicki, M.; Tomaszewski, Z. *J. Chem. Technol. Biotechnol.* **1993**, *52*, 1257.
(91) Zboril, R. Mechanism of Fe_2O_3 Formation during Thermal Decomposition of $FeSO_4 \cdot 7H_2O$, Ph.D. Thesis, Olomouc, 2000.
(92) Mitra, S. *Applied Mössbauer Spectroscopy, Series: Physics and Chemistry of the Earth*; Pergamon: Oxford, 1992; Vol. 18, pp 67−72, 313−343.
(93) Prasad, T. P.; Rao, K. V. K.; Murty, J. S. *Met., Mater. Process.* **1997**, *9*, 9.
(94) Vissokov, G. P.; Pirgov, P. S. *J. Mater. Sci.* **1996**, *31*, 4007.
(95) Bohacek, J.; Subrt, J.; Hanslik, T. *J. Mater. Sci.* **1993**, *28*, 2827.
(96) Montreal Society for Coatings Technology. *J. Coat. Technol.* **1989**, *61*, 73.
(97) Burkhard, D. J. M. *Solid State Commun.* **1997**, *101*, 903.
(98) Mendoza, E. A.; Sunil, D.; Wolkov, E. *Appl. Phys. Lett.* **1990**, *57*, 209.
(99) Morsi, M. M.; El-Shennawi, A. W. A. *Ceram. Int.* **1993**, *19*, 333.
(100) Mimura, N.; Takahara, I.; Ando, M. *Catal. Today* **1998**, *45*, 61.
(101) Zscherpel, D.; Weiss, W.; Schlogl, R. *Surf. Sci.* **1997**, *382*, 326.
(102) Chang, J. S.; Park, S. E.; Park, M. S. *Chem. Lett.* **1997**, *11*, 1123.
(103) Jiang, K.; Yang, J.; Hu, B.; Yang, X.; Mao, L.; Yuan, Y.; Zhang, G. *Hyperfine Interact.* **1998**, *111*, 45.
(104) Xu, L.; Bao, S.; O'Brian, R. J. *Fuel Sci. Techn. Int.* **1994**, *12*, 1323.
(105) Huang, C. S.; Xu, L.; Davis, B. H. *Fuel Sci. Techn. Int.* **1993**, *11*, 639.
(106) Jung, H.; Thomson, W. J. *J. Catal.* **1993**, *139*, 375.
(107) van der Kraan, A. M. *Hyperfine Interact.* **1998**, *111*, 23.
(108) Baerns, M.; Borchert, H.; Kalthoff, R.; Kässner, P.; Majunke, F. *Stud. Surf. Sci. Catal.* **1992**, *72*, 57.
(109) Sazonov, V. A.; Prokudina, N. A.; Gavrilov, V. Y. *Russ. J. Appl. Chem.* **1997**, *70*, 87.
(110) Kotanigawa, T.; Yokoyama, S.; Yamamoto, M. *Fuel* **1989**, *68*, 618.
(111) Miki, J.; Asanuma, M.; Shikada, T. *Chem. Commun.* **1994**, *14*, 1685.
(112) Miki, J.; Asanuma, M.; Tachibana, Y. *Appl. Catal. A* **1994**, *115*, L1.
(113) Shimokawabe, M.; Furuichi, R.; Ishii, T. *Thermochim. Acta* **1977**, *21*, 273.
(114) Oh Sei, J.; Cook, D. C.; Townsend, H. E. *Hyperfine Interact.* **1998**, *112*, 59.
(115) Fouad, N. E.; Ismail, H. M.; Zaki, M. I. *J. Mater. Sci. Lett.* **1998**, *17*, 27.
(116) Leidheiser, H., Jr.; Music, S. *Corros. Sci.* **1982**, *22*, 1089.
(117) Dünnwald, J.; Otto, A. *Corros. Sci.* **1989**, *29*, 1167.
(118) Turner, J. E.; Hendewerk, M.; Parmeter, J.; Neiman, D.; Somorjai, G. A. *J. Electrochem. Soc.* **1984**, *131*, 1777.
(119) Fujishiro, Y.; Uchida, S.; Sato, T. *Int. J. Inorg. Mater.* **1999**, *1*, 67.
(120) Nakatani, Y.; Matsuoka, M. *Jpn. J. Appl. Phys.* **1982**, *21*, L758.
(121) Nakatani, Y.; Sakai, M.; Matsuoka, M. *Jpn. J. Appl. Phys.* **1983**, *22*, 912.
(122) Matsuoka, M.; Nakatani, Y.; Ohido, H. *Nat. Tech. Rep.* **1978**, *24*, 461.
(123) Fujinami, M.; Ujihira, Y. *J. Mater. Sci.* **1985**, *20*, 1859.
(124) McMichael, R. D.; Shull, R. D.; Swartzendruber, L. J.; Bennett, L. H. *J. Magn. Magn. Mater.* **1992**, *111*, 29.
(125) Günther, L. *Phys. World* **1990**, *3*, 28.
(126) Shön, G.; Simon, U. *Colloid Polym. Sci.* **1995**, *273*, 101.
(127) Nixon, L.; Koval, C. A.; Noble, R. D. *Chem. Mater.* **1992**, *4*, 117.
(128) Grimm, S.; Schultz, M.; Barth, S.; Müller, R. *J. Mater. Sci.* **1997**, *32*, 1083.
(129) Batis-Landoulsi, H.; Vergnon, P. *J. Mater. Sci.* **1983**, *18*, 3399.
(130) Pascal, C.; Pascal, J. L.; Favier, F.; Elidrissi Moubtassim, M. L.; Payen, C. *Chem. Mater.* **1999**, *11*, 141.
(131) Ennas, G.; Musinu, A.; Piccaluga, G.; Zedda, D.; Gatteschi, D.; Sangregorio, C.; Stanger, J. L.; Concas, G.; Spano, G. *Chem. Mater.* **1998**, *10*, 495.
(132) Cannas, C.; Gatteschi, D.; Musinu, A.; Piccaluga, G.; Sangregorio, C. *J. Phys. Chem. B* **1998**, *102*, 7721.
(133) Dormann, J. L.; Viart, N.; Rehspringer, J. L.; Ezzir, A.; Niznansky, D. *Hyperfine Interact.* **1998**, *112*, 89.
(134) Martinez, B.; Roig, A.; Obradors, X.; Mollins, E.; Rouanet, A.; Monty, C. *J. Appl. Phys.* **1996**, *79*, 2580.
(135) Ayyub, P.; Multani, M.; Barma, M.; Palkar, V. R.; Vijayaraghavan, R. *J. Phys. C: Solid State Phys.* **1988**, *21*, 2229.
(136) Heiman, N.; Kazama, N. S. *J. Appl. Phys.* **1979**, *50*, 7633.
(137) van Diepen, A. M.; Popma, T. J. A. *J. Phys. Colloque (Paris) C6* **1976**, *37*, 755.
(138) van Diepen, A. M.; Popma, T. J. A. *Solid State Commun.* **1978**, *27*, 121.
(139) Pankhurst, Q. A.; Pollard, R. J. Applied Field Mössbauer Spectroscopy of Magnetic Powders. In *Mössbauer Spectroscopy Applied to Magnetism and Materials Science*; Long, G. J., Grandjean, F., Eds.; Plenum Press: New York, 1993; Vol. 1, pp 77−113.
(140) Nowik, I.; Semmler, W.; Molodtsov, S. *Hyperfine Interact.* **1998**, *112*, 77.
(141) Dickson, D. P. E. *Hyperfine Interact.* **1998**, *111*, 171.
(142) Catlow, C. R.; Corish, J.; Hennesy, J.; Mackrodt, W. C. *J. Am. Ceram. Soc.* **1988**, *71*, 42.
(143) Bowen, L. H.; de Grave, E.; Vandenberghe, R. E. Mössbauer Effect Studies of Magnetic Soils and Sediments. In *Mössbauer Spectroscopy Applied to Magnetism and Materials Science*; Long, G. J., Grandjean, F., Eds.; Plenum Press: New York, 1993; Vol. 1, pp 132−141.
(144) Syvinski, W.; McCarthy, G. North Dakota State University, Fargo, ND, ICDD Grant-in-Aid, 1990.
(145) Fysh, S. A.; Clark, P. E. *Phys. Chem. Miner.* **1982**, *8*, 257.
(146) Vandenberghe, R. E.; de Grave, E.; Landuydt, C.; Bowen, L. H. *Hyperfine Interact.* **1990**, *53*, 175.
(147) Murad, E.; Schwertmann, U. *Clay. Clay Miner.* **1986**, *34*, 1.
(148) Rancourt, D. G.; Julian, S. R.; Daniels, J. M. *J. Magn. Magn. Mater.* **1985**, *49*, 305.
(149) Dormann, J. L.; Cui, J. R.; Sella, C. *J. Appl. Phys.* **1985**, *57*, 4283.
(150) Bentzen, M. D.; van Wonterghem, J.; Morup, S.; Thölen, A.; Koch, C. J. W. *Philos. Mag. B* **1989**, *60*, 169.
(151) Rancourt, D. G.; Daniels, J. M. *Phys. Rev. B* **1984**, *29*, 2410.
(152) Jing, J.; Zhao, F.; Yang, X.; Gonser, U. *Hyperfine Interact.* **1990**, *54*, 571.
(153) de Grave, E.; de Bakker, P. M. A.; Bowen, L. H.; Vandenberghe, R. E. *Z. Pflanzenernähr. Bodenk.* **1992**, *155*, 467.
(154) Schwertmann, U.; Cornell, R. M. *Iron Oxides in the Laboratory, Preparation and Characterization*; VCH: Weinheim, 1991; pp 101−108.
(155) Sapieszko, R. S.; Matijevic, E. *J. Colloid Interface Sci.* **1980**, *74*, 405.
(156) Remy, H. *Lehrbuch der Anorganischen Chemie, Band 2*; Akademische Verlagsgesellschaft Geest & Portig K.-G.: Leipzig, 1959; p 286.
(157) Ben-Dor, L.; Fischbein, E.; Felner, I.; Kalman, Z. *J. Electrochem. Soc.* **1977**, *124*, 451.
(158) Muruyama, T.; Kanagawa, T. *J. Electrochem. Soc.* **1996**, *143*, 1675.
(159) Gonzales-Carreno, T.; Morales, M. P.; Serna, C. J. *J. Mater. Sci. Lett.* **1994**, *13*, 381.
(160) Bauminger, E. R.; Ben-Dor, L.; Felner, I.; Fischbein, E.; Nowik, I.; Ofer, S. *Physica B* **1977**, *86−88*, 910.
(161) Ben-Dor, L.; Fischbein, E. *Acta Crystallogr. B* **1976**, *32*, 667.

(162) Wiarda, D.; Wenzel, T.; Uhrmacher, M.; Lieb, K. P. *J. Phys. Chem. Solids* **1992**, *53*, 1199.
(163) Wiarda, D.; Weyer, G. *Int. J. Mod. Phys. B* **1993**, *7*, 353.
(164) Nakamori, T.; Shibuya, A. *Jpn. Kokai Tokkyo Koho* 1990, 3 pp, patent.
(165) van Hien, N.; Kolchanov, V. A.; Ryzhonkov, D. I.; Filipov, S. I. *Izv. Vyssh. Ucheb. Zaved., Chern. Met.* **1971**, *14*, 5.
(166) Syvinski, W.; McCarthy, G. North Dakota State University, Fargo, ND, ICDD Grant-in-Aid, 1990.
(167) Mørup, S.; Bødker, F.; Hendriksen, P. V.; Linderoth, S. *Phys. Rev. B* **1995**, *52*, 287.
(168) Mørup, S.; Oxborrow, C. A.; Hendriksen, P. V.; Pedersen, M. S.; Hanson, M.; Johansson, C. *J. Magn. Magn. Mater.* **1995**, *140*−*144*, 409.
(169) Tronc, E.; Jolivet, J. P.; Livage, J. *Hyperfine Interact.* **1990**, *54*, 737.
(170) Morris, R. V.; Lauer, H. V., Jr.; Lawson, C. A.; Gibson, E. K., Jr.; Nace, G. A.; Stewart, C. *J. Geophys. Res.* **1985**, *90*, 3126.
(171) Serna, C. J.; Bødker, F.; Mørup, S.; Morales, M. P.; Sandiumenge, F.; Veintemillas-Verdaguer, S. *Solid State Commun.* **2001**, *118*, 437.
(172) Gillot, B.; Nouaim, H.; Mathieu, F. *Mater. Chem. Phys.* **1991**, *28*, 389.
(173) Schwertmann, U.; Fechter, H. *Soil. Sci. Soc. Am. J.* **1984**, *48*, 1462.
(174) Kikkawa, S.; Kanamaru, F.; Koizumi, M. *Inorg. Chem.* **1976**, *15*, 2195.
(175) Taylor, R. M.; Schwertmann, U. *Clay Miner.* **1974**, *10*, 289.
(176) Robl, R. *Angew. Chem.* **1958**, *70*, 367.
(177) Davey, P. T.; Scott, T. R. *Nature* **1957**, *182*, 1363.
(178) Tronc, E.; Chanéac, C.; Jolivet, J. P. *J. Solid State Chem.* **1998**, *139*, 93.
(179) Forestier, H.; Guiot-Guillain, G. *C. R. Acad. Sci. (Paris)* **1934**, *199*, 720.
(180) Dézsi, I.; Coey, J. M. D. *Phys. Status Solidi A* **1973**, *15*, 681.
(181) Trautmann, J. M.; Forestier, H. *C. R. Acad. Sci. (Paris)* **1965**, *261*, 4423.
(182) Reid, A. F.; Ringwood, A. E. *J. Geophys. Res.* **1969**, *74*, 3238.
(183) Yagi, T.; Akimoto, S. In *High-Pressure Research in Geophysisc*; Akimoto, S., Manghnam, M. H., Eds.; Center. Acad. Publ.: Tokyo, 1982; p 81.
(184) Suzuki, T.; Yagi, T.; Akimoto, S.; Ito, A.; Morimoto, S.; Syono, Y. In *Solid State Physics under Pressure*; Minomura, S., Ed.; KKT Scient. Publ.: Tokyo, 1985; p 149.
(185) Syono, Y.; Ito, A.; Morimoto, S.; Suzuki, T.; Yagi, T.; Akimoto, S. *Solid State Commun.* **1984**, *50*, 97.
(186) Nasu, S.; Kurimoto, K.; Nagatomo, S.; Endo, S.; Fujita, F. E. *Hyperfine Interact.* **1986**, *29*, 1583.
(187) Kurimoto, K.; Nasu, S.; Nagatomo, S.; Endo, S.; Fujita, F. E. *Physica B* **1986**, *139/140*, 495.
(188) Staun Olsen, J.; Cousins, C. S. G.; Gerward, L.; Jhans, H.; Sheldon, B. J. *Phys. Scripta* **1991**, *43*, 327.
(189) Howard, D. G.; Nussbaum, R. H. *Surf. Sci.* **1980**, *93*, L105.

CM0111074